

Superfluid states in α-T_3 lattice

Yu-Rong Wu(吴玉容) and Yi-Cai Zhang(张义财)

Citation: Chin. Phys. B, 2021, 30 (**6**): 060306. DOI: 10.1088/1674-1056/abea8a
Journal homepage: http://cpb.iphy.ac.cn; http://iopscience.iop.org/cpb

What follows is a list of articles you may be interested in

Dynamics of bright soliton in a spin-orbit coupled spin-1 Bose-Einstein condensate

Hui Guo(郭慧), Xu Qiu(邱旭), Yan Ma(马燕), Hai-Feng Jiang(姜海峰), and Xiao-Fei Zhang(张晓斐)
Chin. Phys. B, 2021, 30 (**6**): 060310. DOI: 10.1088/1674-1056/abf34a

Dynamical stability of dipolar condensate in a parametrically modulated one-dimensional optical lattice

Ji-Li Ma(马吉利), Xiao-Xun Li(李晓旬), Rui-Jin Cheng(程瑞锦), Ai-Xia Zhang(张爱霞), and Ju-Kui Xue(薛具奎)
Chin. Phys. B, 2021, 30 (**6**): 060307. DOI: 10.1088/1674-1056/abd746

Ultradilute self-bound quantum droplets in Bose-Bose mixtures at finite temperature

Jia Wang(王佳), Xia-Ji Liu(刘夏姬), and Hui Hu(胡辉)
Chin. Phys. B, 2021, 30 (**1**): 010306. DOI: 10.1088/1674-1056/abd2ad

Interference properties of two-component matter wave solitons

Yan-Hong Qin(秦艳红), Yong Wu(伍勇), Li-Chen Zhao(赵立臣), Zhan-Ying Yang(杨战营)
Chin. Phys. B, 2020, 29 (**2**): 020303. DOI: 10.1088/1674-1056/ab65b7

Collapses-revivals phenomena induced by weak magnetic flux in diamond chain

Na-Na Chang(常娜娜), Wen-Quan Jing(景文泉), Yu Zhang(张钰), Ai-Xia Zhang(张爱霞), Ju-Kui Xue(薛具奎), Su-Peng Kou(寇谡鹏)
Chin. Phys. B, 2020, 29 (**1**): 010306. DOI: 10.1088/1674-1056/ab6087

Superfluid states in α–T_3 lattice*

Yu-Rong Wu(吴玉容) and Yi-Cai Zhang(张义财)†

School of Physics and Materials Science, Guangzhou University, Guangzhou 510006, *China*

(Received 4 December 2020; revised manuscript received 5 February 2021; accepted manuscript online 1 March 2021)

The superfluid states of attractive Hubbard model in α–T_3 lattice are investigated. It is found that one usual needs three non-zero superfluid order parameters to describe the superfluid states due to three sublattices. When two hopping amplitudes are equal, the system has particle–hole symmetry. The flat band plays an important role in superfluid pairing near half filling. For example, when the filling factor falls into the flat band, the large density of states in the flat band favors superfluid pairing and the superfluid order parameters reach relatively large values. When the filling factor is in the gap between the flat band and upper band, the superfluid order parameters take small values due to the vanishing of density of states. The superfluid order parameters show nonmonotonic behaviors with the increase of filling factor. At last, we also investigate the edge states with open boundary conditions. It is shown that there exist some interesting edge states in the middle of quasi-particle bands.

Keywords: superfluid states, flat band, α–T_3 lattice, particle–hole symmetry

PACS: 03.75.Kk, 67.85.Lm, 71.10.Fd, 74.20.–z **DOI:** 10.1088/1674-1056/abea8a

1. Introduction

The discovery of graphene has great significance in the developments of condensed matter physics. Graphene was first proposed in 1947,[1] and Novoselv and Geim experimentally prepared it in 2004.[2] Graphene is a two-dimensional material composed of carbon atoms which are arranged in a hexagonal to form a honeycomb lattice. In graphene, Dirac-Weyl Hamiltonian with pseudospin $S = 1/2$ can be used to describe its low-energy behaviors.[3–5] The interests in graphene are largely due to its unique band structures and massless low-energy excitation.[6–8]

For researchers, it is interesting to find new two-dimensional materials similar to graphene. The honeycomb lattice structure of graphene provides a favorable reference for the study of other new models. Adding an atom to the center of nonequivalent "rim" sites on the hexagon gives a dice lattice.[9–12] The low-energy excitation of the dice lattice is also described by the Dirac equation, but its pseudospin $S = 1$ instead of $1/2$. The dice lattice can be realized with two different schemes: one is to fabricate the trilayer structure of cubic lattice (e.g., $SrTiO_3/SrIrO_3/SrTiO_3$) in the (111) direction.[13,14] Alternatively, it is convenient to use the cold atoms in optical lattice.[15–17] The α–T_3 lattice is essentially a hybrid between graphene and dice lattice,[18–20] parameter α is used to represent the hopping strength between the hexagonal center and rim atoms.[21–23] When α is 0, the lattice becomes graphene, and if α is 1, it means that the hopping amplitudes between the central atom and one of the hexagonal atoms are equal, then it is the dice lattice. Compared with graphene, the band structure of the α–T_3 lattice has a distinguishing characteristic. In addition to the conduction band and valence band $E_{\pm}(k)$, there is a flat band $E_0(k)$ in the middle, which is similar to that of the dice lattice. For this kind of novel material, researchers have done a lot of works on it, for example, Hofstadter butterfly effect,[27] magneto-optical conductivity,[24–26] Klein tunneling,[28–30] zitterbewegung effect,[31] magnetism,[32,33] magnetoconductivity,[34–36] etc.

The superfluidity of dipolar excitons in double-layer α–T_3 lattice under strong magnetic field has been studied.[37] Inspired by the superfluid phases for bosons in dice lattice,[38] the superfluidity for fermions in α–T_3 is studied in this paper. As far as we know, the literature on the superfluid states of fermions in the α–T_3 lattice is comparatively sparse. It is expected that the dispersionless flat band would play an important role in the formations of superfluid states. In this work, we study the Fermi Hubbard model with attractive interactions in α–T_3 lattice. In specific, with the mean-field method, we obtain the superfluid order parameters (pairing gaps in superconductor) through solving the self-consistent equations. And then we carefully analyze the evolutions of the superfluid order parameters under the variations of the model parameters. It is found that the Hamiltonian has particle–hole symmetry under certain conditions. Near half-filling, in comparison with the usual two-band system, e.g., Haldane model, the large density of states of the flat band in the α–T_3 lattice is in favor of the superfluid states. The superfluid order parameters also show non-monotonic behaviors as the filling factor increases. In addition, there exist some interesting edge states on the boundaries of a lattice ribbon.

*Project supported by the National Natural Science Foundation of China (Grant No. 11874127) and the startup grant from Guangzhou University.

†Corresponding author. E-mail: zhangyicai123456@163.com

© 2021 Chinese Physical Society and IOP Publishing Ltd

The paper is organized as following. In Section 2, we give the α–T_3 Hubbard model Hamiltonian. The mean-field theory is reviewed briefly in Section 3. In Section 4, we firstly discuss the particle–hole symmetry of the system, and then analyze the superfluid order parameters of the α–T_3 lattice. In Section 5, we turn to the discussions on the edge states. Finally, we give the summary in Section 6.

2. The α–T_3 Hubbard model Hamiltonian

Hubbard model is an important model in condensed matter physics, which can be used to describe metal–insulator transition,[39–41] magnetic phase transition,[42] and superfluid–insulator transition.[43–45] The spatial structure of α–T_3 lattice is shown in Fig. 1. A unit cell consists of three different lattice sites (A, B, and C), in which sites A and B are located at the vertices of a hexagon to form a honeycomb lattice, and site C is located at the center of the hexagon. The hopping amplitude $t_{\rm AB} = t_1 = t$ between A and B sites. In particular, C sites are only linked to B sites with hopping strength $t_{\rm BC} = t_2 = \alpha t_1$ with $\alpha \geq 0$. In this paper, we consider two-component Fermi gases with spin $\sigma = \uparrow, \downarrow$, which interact through attractive interaction $-U$ ($U > 0$). In cold atom experiments, the interactions strength U can be tuned by a magnetic field. The α–T_3 Hubbard model Hamiltonian reads

$$\begin{aligned}\mathcal{H} &= \sum_{ij\sigma} t_{ij} c^{\dagger}_{i\sigma} c_{j\sigma} + M\left(\sum_{i\sigma} n_{i{\rm A}\sigma} - \sum_{i\sigma} n_{i{\rm C}\sigma}\right) \\ &\quad - \mu \sum_{i\sigma} n_{i\sigma} - U \sum_{i} n_{i\uparrow} n_{i\downarrow} \\ &= H_0 - U \sum_{i} n_{i\uparrow} n_{i\downarrow}, \end{aligned} \tag{1}$$

where t_{ij} is the hopping amplitude between sublattices and μ describes the chemical potential. Noted that, M is the energy offset between sublattices A and C,[46] and $n_{i\sigma} = c^{\dagger}_{i\sigma} c_{i\sigma}$ denotes the particle number operator for spin component σ at site i. H_0 is the non-interacting part of the Hamiltonian. Furthermore, we use i to label the unit cell, the creation operators of three states in corresponding sublattices are represented by $a^{\dagger}_i$, $b^{\dagger}_i$, and $c^{\dagger}_i$, respectively. In the following, we only consider the nearest neighbor hopping, and assume $t_{\rm AB} = t_{\rm BA} = t_1$, $t_{\rm BC} = t_{\rm CB} = t_2$ are all real. Under periodic boundary condition , using the Fourier transform, i.e., $a(b/c)_i = 1/\sqrt{N}\sum a(b/c)(\boldsymbol{k})\, {\rm e}^{{\rm i}\boldsymbol{k}\cdot\boldsymbol{r}_i}$ (N is the number of unit cells and $\boldsymbol{r}_i$ is the position vector of site i), it is convenient to obtain the non-interacting Hamiltonian (not including the U term) in momentum space

$$\mathcal{H}_0(\boldsymbol{k}) = \psi^{\dagger}(\boldsymbol{k}) \boldsymbol{h}(\boldsymbol{k}) \psi(\boldsymbol{k}), \tag{2}$$

where $\psi^{\dagger}(\boldsymbol{k}) = [a^{\dagger}_{\sigma}(\boldsymbol{k}), b^{\dagger}_{\sigma}(\boldsymbol{k}), c^{\dagger}_{\sigma}(\boldsymbol{k})]$ and

$$\boldsymbol{h}(\boldsymbol{k}) = \begin{bmatrix} M-\mu & h_{12}(\boldsymbol{k}) & 0 \\ h_{21}(\boldsymbol{k}) & -\mu & h_{23}(\boldsymbol{k}) \\ 0 & h_{32}(\boldsymbol{k}) & -M-\mu \end{bmatrix} \tag{3}$$

with $h_{12}(\boldsymbol{k}) = t_1 \sum_{\delta} \cos(\boldsymbol{k}\cdot\boldsymbol{a}_{\delta}) + {\rm i}t_1 \sum_{\delta} \sin(\boldsymbol{k}\cdot\boldsymbol{a}_{\delta})$, $h_{21}(\boldsymbol{k}) = h^{*}_{12}(\boldsymbol{k})$, $h_{23}(\boldsymbol{k}) = t_2 \sum_{\delta} \cos(\boldsymbol{k}\cdot\boldsymbol{b}_{\delta}) + {\rm i}t_2 \sum_{\delta} \sin(\boldsymbol{k}\cdot\boldsymbol{b}_{\delta})$, $h_{32}(\boldsymbol{k}) = h^{*}_{23}(\boldsymbol{k})$, and $\boldsymbol{k} = (k_x, k_y)$. Specifically, the two-dimensional vectors $\boldsymbol{a}_{\delta}$ and $\boldsymbol{b}_{\delta}$ are shown in Fig. 1. In the following, we take $t_1 = 1$ as the energy unit. The single-particle Hamiltonian H_0 has three energy bands, and there exists a flat band in the middle (see Fig. 2).

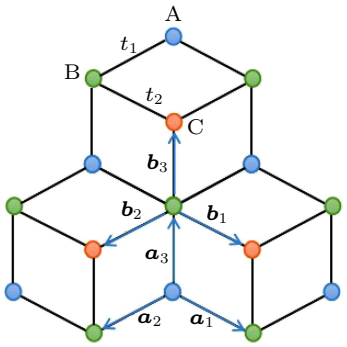


Fig. 1. Schematic diagram of α–T_3 lattice. Sublattices A, B, and C are shown in blue, green, and red, respectively. The vectors $\boldsymbol{b}_1 = \boldsymbol{a}_1 = [\sqrt{3}/2, -1/2]$, $\boldsymbol{b}_2 = \boldsymbol{a}_2 = [-\sqrt{3}/2, -1/2]$, and $\boldsymbol{b}_3 = \boldsymbol{a}_3 = [0, 1]$ with lattice spacing $a = 1$.

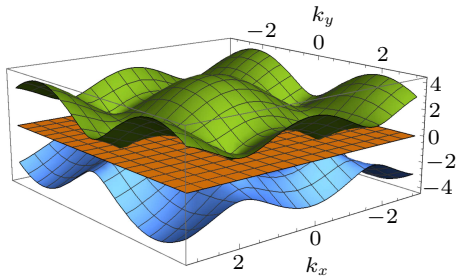


Fig. 2. Three single-particle energy bands in α–T_3 lattice with $t_2 = t_1 = 1$, $\mu = 0$, and $M = 0$. The flat band is in middle of upper and lower bands.

3. Mean-field theory

In the presence of the interaction between the opposite spins, we use the mean field decoupling to solve the Hamiltonian and select $\Delta_i = -U\langle c_{i\downarrow} c_{i\uparrow}\rangle$ as the superfluid order parameter (pairing gap). When $M \neq 0$, the Bogoliubov–de Gennes Hamiltonian in momentum space is

$$\mathcal{H}_{\rm BdG} = \sum_{\boldsymbol{k}} \Psi^{\dagger}(\boldsymbol{k}) H_{\rm BdG}(\boldsymbol{k}) \Psi(\boldsymbol{k}) \tag{4}$$

with $\Psi^{\dagger}(\boldsymbol{k}) = [a^{\dagger}_{\uparrow}(\boldsymbol{k}), b^{\dagger}_{\uparrow}(\boldsymbol{k}), c^{\dagger}_{\uparrow}(\boldsymbol{k}), a_{\downarrow}(-\boldsymbol{k}), b_{\downarrow}(-\boldsymbol{k}), c_{\downarrow}(-\boldsymbol{k})]$,

$$H_{\rm BdG} = \begin{bmatrix} M-\mu & h_{12}(\boldsymbol{k}) & 0 & \Delta_{\rm A} & 0 & 0 \\ h_{21}(\boldsymbol{k}) & -\mu & h_{23}(\boldsymbol{k}) & 0 & \Delta_{\rm B} & 0 \\ 0 & h_{32}(\boldsymbol{k}) & -M-\mu & 0 & 0 & \Delta_{\rm C} \\ \Delta^{*}_{\rm A} & 0 & 0 & -M+\mu & -h^{*}_{12}(-\boldsymbol{k}) & 0 \\ 0 & \Delta^{*}_{\rm B} & 0 & -h^{*}_{21}(-\boldsymbol{k}) & \mu & -h^{*}_{23}(-\boldsymbol{k}) \\ 0 & 0 & \Delta^{*}_{\rm C} & 0 & -h^{*}_{32}(-\boldsymbol{k}) & M+\mu \end{bmatrix}. \tag{5}$$

By using the Bogoliubov transformation, the eigenenergies $E^{{\rm p(h)}1,2,3}(\boldsymbol{k})$ can be easily obtained. It is important to emphasize that the BdG Hamiltonian obeys the particle–hole symmetry, p (h) corresponds to the particle (hole) and 1, 2, 3 represent three branches of excitation due to the sublattices A,

B, and C. With the particle–hole symmetry of $H_{\rm BdG}$, one can show that $E^{\rm h1,2,3}(\boldsymbol{k}) = -E^{\rm p1,2,3}(-\boldsymbol{k})$,[47] and in the ground state, the thermodynamic potential per unit cell is given by

$$\Omega = \frac{1}{N}\sum_{\boldsymbol{k}}[-|E^{\rm p1}(\boldsymbol{k})| - |E^{\rm p2}(\boldsymbol{k})| - |E^{\rm p3}(\boldsymbol{k})| - 3\mu] + \frac{(\Delta_{\rm A}^2 + \Delta_{\rm B}^2 + \Delta_{\rm C}^2)}{U}. \tag{6}$$

The pairing gaps can be solved by $\partial\Omega/\partial\Delta_{\rm A,B,C} = 0$, and the chemical potential can be obtained from $n = -\partial\Omega/\partial\mu$. The resultant four equations for $\Delta_{\rm A,B,C}$ and μ are solved by numerical methods.

4. Particle–hole symmetry and numerical results

First of all, we carefully analyze the particle–hole symmetry (note here that the particle–hole symmetry is different from the one of the BdG Hamiltonian discussed in Section 3) in the case of $t_2 = t_1$. Applying the particle–hole transformation to the system,[43,48]

$$a_{i\sigma} \to \tilde{a}^{\dagger}_{i\sigma},\ \ b_{i\sigma} \to -\tilde{b}^{\dagger}_{i\sigma},\ \ c_{i\sigma} \to \tilde{c}^{\dagger}_{i\sigma},$$
$$a^{\dagger}_{i\sigma} \to \tilde{a}_{i\sigma},\ \ b^{\dagger}_{i\sigma} \to -\tilde{b}_{i\sigma},\ \ c^{\dagger}_{i\sigma} \to \tilde{c}_{i\sigma}, \tag{7}$$

in the case of $M = 0$ and the chemical potential $\mu = 0$, the Hamiltonian remains invariant at half-filling (3 particles per unit cell). Nevertheless, for $M \neq 0$, in order to keep the Hamiltonian unaltered, the inversion transformation $\boldsymbol{r} \to -\boldsymbol{r}$ and the exchange of A and C sublattices are needed. In this sense, the Hamiltonian has particle–hole symmetry. In the following, we only consider the case of the number of particles $n > 3$ per unit cell ($n = 3$ is half-filling, i.e., there are three particles in a unit cell). Further more, similar to the Haldane–Hubbard model,[43] one can show that, for the cases of $\Delta n \equiv n - 3 > 0$ and $-\Delta n < 0$, the chemical potential and superfluid order parameters satisfy the relationship

$$\mu(-\Delta n) = -\mu(\Delta n),\ \ \Delta_{\rm A}(-\Delta n) = \Delta_{\rm C}(\Delta n),$$
$$\Delta_{\rm C}(-\Delta n) = \Delta_{\rm A}(\Delta n). \tag{8}$$

The above equations show that, when it is at the half-filling ($\Delta n = 0$), the chemical potential is exactly zero and $\Delta_{\rm A} = \Delta_{\rm C}$.

When M, t_1, and t_2 take some specific values, it is found that $\Delta_{\rm A(B,C)}$ are always real. The evolutions of the mean-field superfluid order parameters and chemical potential with attractive interaction U are depicted in Figs. 3 and 4. It is shown that, on the whole, $\Delta_{\rm A(B,C)}$ and μ increase when the interaction U becomes strong. In contrast with the usual two-band system, for example, Haldane model, the presence of flat band plays an important role in superfluid pairing, especially for half filling. In the Haldane model and at the half filling, when the attractive interaction is weak, the system also remains in an insulator phase. Only when the interaction is large enough, the system develops some non-vanishing superfluid order parameters.[43] While for the α–T_3 lattice, because of the presence of flat band, when it is half filling, the system is in a metal state. Once the attractive interaction is turned on, the system gets some nonzero superfluid order parameters.

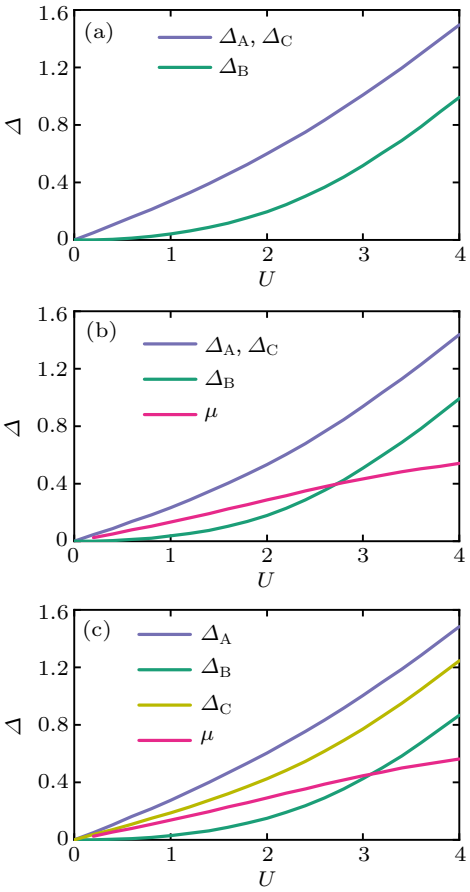


Fig. 3. The superfluid order parameters as functions of interaction U ($M = 0$) (a) at half-filling with $\mu = 0$, $t_1 = t_2 = 1$; (b) the average number of particles $n = 3.5$, $\mu \neq 0$ with $t_2 = t_1 = 1$; (c) $n = 3.5$, $\mu \neq 0$ and the hopping amplitude $t_1 = 1$, $t_2 = 1.2$.

For $M = 0$, the Hamiltonian is subject to the inverse symmetry, there are two different situations: (1) Dice lattice ($t_2 = t_1$), due to the equivalence between sublattices A and C, whether it is at half-filling or not, $\Delta_{\rm A}$ is the same as $\Delta_{\rm C}$ but differs from $\Delta_{\rm B}$ [Figs. 3(a) and 3(b)], and $\Delta_{\rm B}$ is smaller than $\Delta_{\rm A(C)}$; (2) α–T_3 lattice ($t_2 \neq t_1$), Δ differs for three sublattices A, B, and C [Fig. 3(c)]. The $\Delta_{\rm C}$ lies in between $\Delta_{\rm A}$ and $\Delta_{\rm B}$.

When $M \neq 0$, the Hamiltonian does not obey the inversion symmetry and the roles of sublattices A and C are not equivalent. Nevertheless, the Hamiltonian has particle–hole symmetry when it is half-filling and $t_2 = t_1$. (3) Dice lattice ($t_1 = t_2$) and at half-filling, the situation of $\Delta_{\rm A(B,C)}$ is similar as the case (1) discussed above, but $\Delta_{\rm B}$ is larger than $\Delta_{\rm A(C)}$ [Fig. 4(a)]. Here $\Delta_{\rm A} = \Delta_{\rm C}$ is a consequence of the particle–hole symmetry as discussed above. When it is at half-filling, after exchanging sublattices A and C, the Hamiltonian is not changed. Consequently the superfluid order parameters are

equal, i.e., $\Delta_A = \Delta_C$. (4) Above the half-filling, both dice lattice and α–T_3 lattice yield three different superfluid order parameters which are similar to case (2). However, for the dice lattice, Δ_B is greater than Δ_A and Δ_C [Fig. 4(b)]. For the α–T_3 lattice, Δ_C is always the smallest one. When the value of U is small, there is a little difference between Δ_A and Δ_B. When $3.190 > U > 0.616$, Δ_B is greater than Δ_A, but the situation is reversed at $U \approx 3.190$, and Δ_B becomes smaller than Δ_A [Fig. 4(c)].

In Figs. 5 and 6, we report the evolutions of superfluid order parameter Δ and chemical potential μ as the filling factor increases for different interaction strength U. It is found that, for the whole range of filling $3 \leq n \leq 6$, the order parameters increase with the interaction strength. When the filling factor falls into the flat band, i.e., $3 < n < 4$, and $M = 0$, the superfluid order parameters take relatively larger values for a fixed interaction strength (see Fig. 5). This is because the large density of states of the flat band favors the superfluid pairing. When the filling factor n crosses the flat band ($n \geq 4$), the chemical potential displays a jump due to discontinuous of density of states (especially when the interaction is weak) (see Figs. 5(a) and 5(b)). Similarly, the small density of states between the flat band and upper band also causes a dip in the order parameters (see Fig. 6). When $M = 0$, on the whole, the superfluid order parameters become smaller as the filling factor increases. However, when $M \neq 0$, the superfluid order parameters can reach relatively large values, especially for strong interaction and large filling factor (see Figs. 6(c) and 6(d)). When the filling factor approaches its maximum possible value ($n = 6$), the system becomes a band insulator and the superfluid order parameters are vanishing. Figures 5 and 6 also show that the superfluid order parameter for sublattice A is always larger than that of sublattice C, i.e., $\Delta_A > \Delta_C$. In addition, when the inversion symmetry is broken ($M \neq 0$), the superfluid order parameters show some nonmonotonic behaviors as the filling factor increases (see Fig. 6).

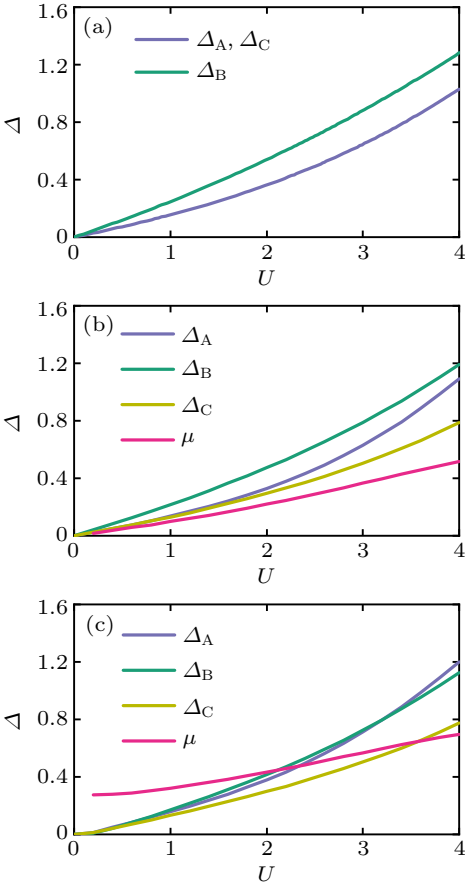


Fig. 4. The evolutions of superfluid order parameters with interaction U ($M = 2$) (a) at half-filling with $\mu = 0$, $t_1 = t_2 = 1$; (b) the average number of particles $n = 3.5$, $\mu \neq 0$ but $t_2 = t_1 = 1$; (c) $n = 3.5$, $\mu \neq 0$ and the hopping amplitude $t_1 = 1$, $t_2 = 1.2$.

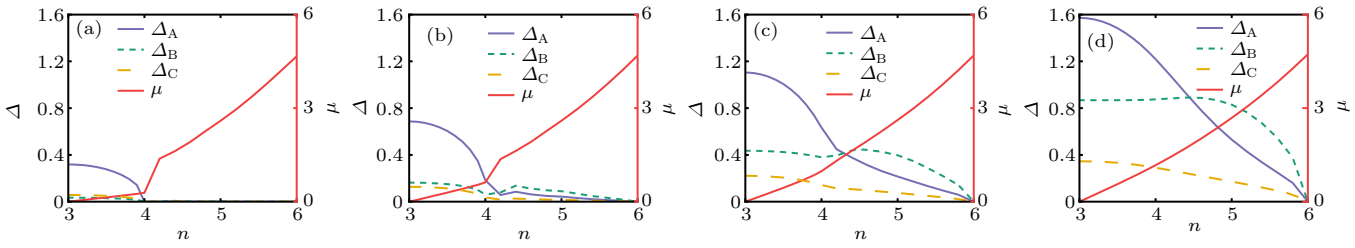


Fig. 5. The evolutions of the superfluid order parameters and chemical potential with filling factor ($M = 0$, $t_2 = 1.2t_1 = 1.2$). (a) Interaction $U = 1$, (b) $U = 2$, (c) $U = 3$, and (d) $U = 4$.

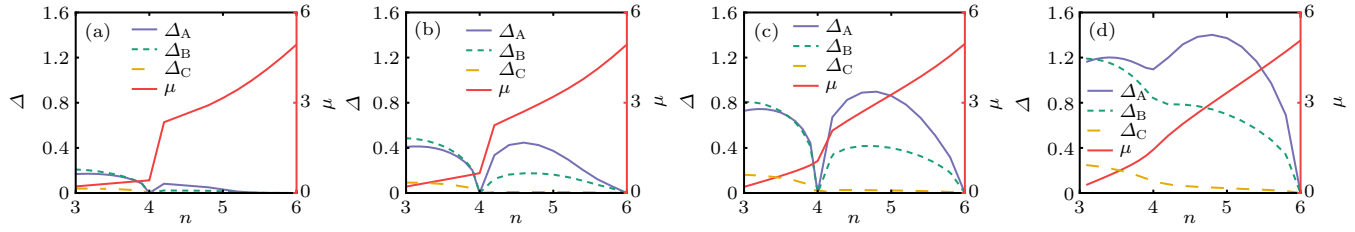


Fig. 6. The evolutions of the superfluid order parameters and chemical potential($M = 2$, $t_2 = 1.2t_1 = 1.2$. (a) Interaction $U = 1$, (b) $U = 2$, (c) $U = 3$, and (d) $U = 4$.

5. Edge states

In this section, we analyze the edge states of the system under periodic boundary conditions in y-direction and open boundary conditions in x-direction with B–B edges.[26] From left-hand to right-hand side, the lattice sites are arranged like BACBAC$\cdots$BACB with 20 complete spatial periods.

In the absence of interaction and $M = 0$, there exist two degenerate edge states,[26] and one locates at the left-hand edge, while the other one is on the right-hand edge. When $M \neq 0$, similarly as gapped graphene case, the existence of edge states can be understood as midgap states near a domain wall.[46,49] Similar as the gapped graphene, the Dirac Hamiltonian (for one of two Dirac cones) of the edge state is

$$H_{\text{Dirac}} = \begin{pmatrix} m(x) & -vk - \mathrm{i}vq & 0 \\ -vk + \mathrm{i}vq & 0 & -vk - \mathrm{i}vq \\ 0 & -vk + \mathrm{i}vq & -m(x) \end{pmatrix}, \tag{9}$$

where $\lim_{x\to\infty} m(x) \to M > 0$ and $\lim_{x\to-\infty} m(x) \to -M < 0$. Here Fermi velocity $v = 3ta/2$, momentum k is a real number for y-direction, the momentum operator for x-direction $q = -\mathrm{i}\partial_x$. The wave function (non-normalized) of the edge state near the left-hand boundary is

$$\psi_k(x) = \begin{pmatrix} 1 \\ -\sqrt{2} \\ 1 \end{pmatrix} \mathrm{e}^{-\int_0^x \frac{m(z)}{\sqrt{2}}\,\mathrm{d}z} = \begin{pmatrix} 1 \\ -\sqrt{2} \\ 1 \end{pmatrix} \mathrm{e}^{-\frac{Mx}{\sqrt{2}}} \tag{10}$$

with energy $E = \sqrt{2}vk$.

When superfluid order parameters $\Delta \neq 0$, one needs to introduce freedoms for hole's part to describe the edge states. In such a situation, the wave functions for particle's and hole's parts would couple. The edge states are reported in Figs. 7–9. When the Hamiltonian has particle–hole symmetry ($n = 3$, $\mu = 0$, and $t_2 = t_1$), for every lattice momentum k, there also exist two degenerate edge states (not shown in Fig. 7), which locate respectively at the left-hand and right-hand boundaries. In such a case, the two edge states are related to each other through a particle–hole symmetry, which includes inversion transformation $\boldsymbol{r} \to -\boldsymbol{r}$ and the exchange of A and C sublattices as discussed in Section 4.

When the particle–hole symmetry is broken, for example, the filling is away from half filling (chemical potential $\mu \neq 0$) or $t_2 \neq t_1$, the degeneracy of two edge states (energy $E_i > 0$) is removed (see Figs. 7(a) and 7(b)). As the interaction grows ($U = 0 \to 4$), the edge states near the right-hand boundary are pushed into continuous spectra as shown in Figs. 7(b)–7(d). The wave functions of the two edge states Fig. 7(a) are shown in Fig. 9 with $U = 1$, $M = 2$, $n = 3.5$, $t_2 = 1.2t_1 = 1.2$, and lattice momentum $k = 0$.

It is found that the edge states are localized near the boundaries. Figure 8 shows the evolutions of energy bands and edge states as t_2 increases. It is found that, when t_2 increases, the lowest particle band is getting flat. At the same time, the region of existence of edge states also becomes broader. We note that the energies of the edge states do not cross the zero energy, which is very different from the case of Haldane model.[43] This is because, in the α–T_3 model, the total Chern number of the lower three hole bands is zero. Therefore, the edge states of zero energy could not be guaranteed to exist in this α–T_3 system. While the Chern number is not vanishing in Haldane model for the topological superfluid phase, which supports two edge states of zero energy.

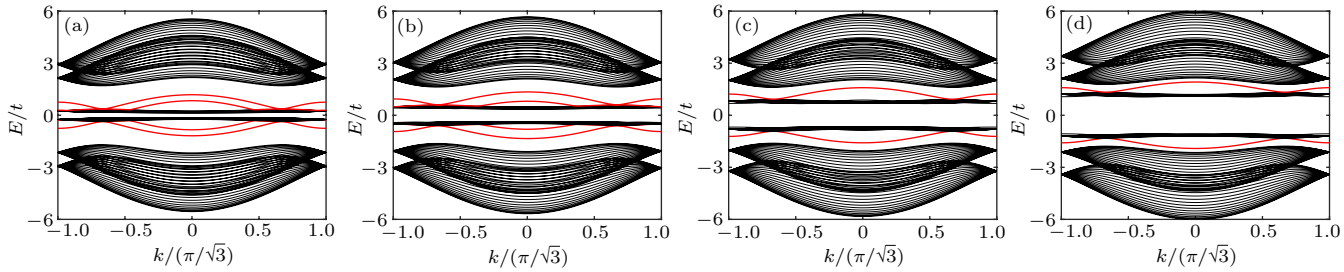


Fig. 7. Energy spectrum and edge states for $M = 2$, $t_2 = 1.2t_1 = 1.2$, $n = 3.5$. (a) $U = 1$, (b) $U = 2$, (c) $U = 3$, (d) $U = 4$. The edge modes in (a)–(d) are plotted in red.

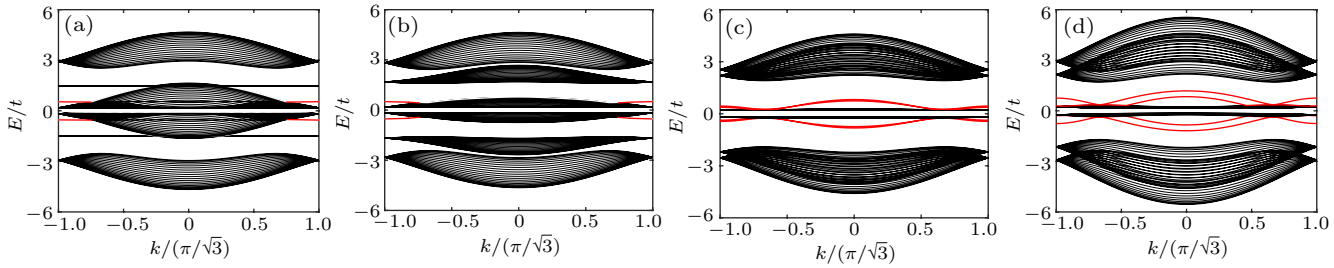


Fig. 8. Energy spectrum and edge states for $M = 2$, $t_1 = 1$, $n = 3.5$, $U = 1$. (a) $t_2 = 0$, (b) $t_2 = 0.4$, (c) $t_2 = 0.8$, (d) $t_2 = 1.2$. The edge modes in (a)–(d) are plotted in red.

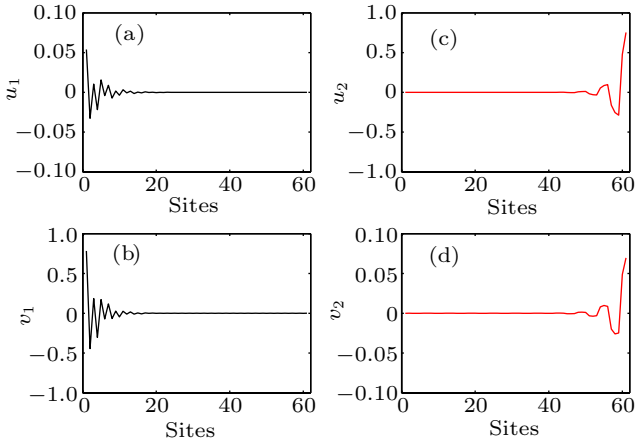


Fig. 9. Wave functions of two edge states (energy $E_i > 0$) in Fig. 7(a) with $U = 1, M = 2, t_2 = 1.2t_1 = 1.2, n = 3.5$, and momentum $k = 0$ (see the red lines in Fig. 7). u_i (v_i) is wave function for the particle (hole) part of the i-th edge state.

6. Summary

In conclusion, we investigate the superfluid states in attractive Hubbard model of α–T_3 lattice. Because there exist three bands, one needs three superfluid order parameters to describe the superfluid states, which is very different from the usual two-band system, e.g., Haldane model or graphene. However, similarly as the Haldane model, the α–T_3 model also has particle–hole symmetry when two hopping amplitudes are equal. It is found that the flat band plays an important role in pairing, especially for the half-filling. We carefully analyze the the evolutions of the superfluid order parameters with the increase of interaction strength and filling factor. In the absence of inversion symmetry, the superfluid order parameters show nonmonotonic behaviors with the increase of filling factor. Finally, it is found that there exist some edge states localized at boundaries of a ribbon with open boundary conditions.

There are some other interesting questions which are worthwhile to further investigations. For example, what are the collective modes in such a multi-band system,[50–52] how is the superfluid density affected by the flat band,[53–55] and how does magnetic field affect the superfluid states.

Acknowledgement

We would like to thank Jun-Feng Liu and Wen-Yu Shan for useful discussions.

References

[1] Wallace P R 1947 *Phys. Rev* **71** 622
[2] Novoselov K S, Geim A K, Morozov S V, Jiang D, Zhang Y, Dubonos S V, Grigorieva I V and Firsov A A 2004 *Science* **306** 666
[3] Novoselov K S, Geim A K, Morozov S V, Jiang D, Katsnelson M I, Grigorieva I V, Dubonos S V and Firsov A A 2005 *Nature* **438** 197
[4] Stander N, Huard B and Goldhaber-Gordon D 2009 *Phys. Rev. Lett.* **102** 026807
[5] Burkov A A, Hook M D and Leon Balents 2011 *Phys. Rev. B* **84** 235126
[6] Malcolm J D and Nicol E J 2016 *Phys. Rev. B* **93** 165433
[7] Schoop L M 2016 *Nat. Commun.* **7** 11696
[8] Xu H Y and Lai Y C 2016 *Phys. Rev. B* **94** 165405
[9] Sutherland B 1986 *Phys. Rev. B* **34** 5208
[10] Julien Vidal, Rémy Mosseri and Benoit Douçot 1998 *Phys. Rev. Lett* **81** 5888
[11] Oriekhov D O, Gorbar E V and Gusynin V P 2018 *Low Temperature Physics* **44** 1313
[12] Gorbar E V, Gusynin V P and Oriekhov D O 2019 *Phys. Rev. B* **99** 155124
[13] Wang F and Ran Y 2011 *Phys. Rev. B* **84** 241103
[14] Okamoto S and Xiao D 2018 *J. Phys. Soc. Jpn.* **87** 041006
[15] Bloch I, Dalibard J and Sylvain 2012 *Nat. Phys.* **8** 267
[16] Bercioux D, Urban D F, Grabert H and Häusler W 2009 *Phys. Rev. A* **80** 063603
[17] Möller G and Cooper N R 2012 *Phys. Rev. Lett.* **108** 045306
[18] Bryenton K R 2018 *Optical Properties of the α–T_3 Semi-Dirac Model* Ph.D. dissertation (Guelph: University of Guelph)
[19] Chen L, Zuber J, Ma Z S and Zhang C 2019 *Phys. Rev. B* **100** 035440
[20] Iurov A, Zhemchuzhna L, Dahal D, Gumbs G and Huang D H 2020 *Phys. Rev. B* **101** 035129
[21] Raoux A, Morigi M, Fuchs J N, Piéchon F and Montambaux G 2014 *Phys. Rev. Lett.* **112** 026402
[22] Alam M W, Souayeh B and Islam S F 2019 *J. Phys.: Condens. Matter* **31** 485303
[23] Wang C Z, Han C D, Xu H Y and Lai Y C 2019 *Phys. Rev. B* **99** 144302
[24] Kovács Á D, Dávid G, Dóra B and Cserti J 2017 *Phys. Rev. B* **95** 035414
[25] Illes E and Nicol E J 2016 *Phys. Rev. B* **94** 125435
[26] Chen Y R, Xu Y, Wang J, Liu J F and Ma Z S 2019 *Phys. Rev. B* **99** 045420
[27] Illes E 2017 *Properties of the α–T_3 Model* Ph.D. dissertation (Guelph: University of Guelph)
[28] Balázs Dóra, Kailasvuori J and Moessner R 2011 *Phys. Rev. B* **84** 195422
[29] Illes E and Nico E J 2017 *Phys. Rev. B* **95** 235432
[30] Urban D F, Bercioux D, Wimmer M and Häusler W H 2011 *Phys. Rev. B* **84** 115136
[31] Biswas T and Ghosh T K 2018 *J. Phys.: Condens. Matter* **30** 075301
[32] Raoux A, Morigi M, Fuchs J N, Piéchon P and Montambaux G 2014 *Phys. Rev. Lett.* **112** 026402
[33] Roslyak O, Gumbs G, Balassis A and Elsayed H 2020 *arXiv:* **2006** 15447
[34] Biswas T and Ghosh T K 2016 *J. Phys.: Condens. Matter* **28** 495302
[35] Islam S F and Dutta P 2017 *Phys. Rev. B* **96** 045418
[36] Biswas T and Ghosh T K 2018 *J. Phys.: Condens. Matter* **30** 075301
[37] Abranyos Y, Berman O L and Gumbs G 2020 *Phys. Rev. B* **102** 155408
[38] Rizzi M, Cataudella V and Fazio R 2006 *Phys. Rev. B* **73** 144511
[39] Tran M T and Kuroki K 2009 *Phys. Rev. B* **79** 125125
[40] Imada M, Fujimori A and Tokura Y 1998 *Phys. Rev. B* **70** 1039
[41] Liu H D 2019 *Chin. Phys. B* **28** 107102
[42] Zheng W, Shen H, Wang Z and Zhai H 2015 *Phys. Rev. B* **91** 161107
[43] Zhang Y C, Xu Z H and Zhang S Z 2017 *Phys. Rev. A* **95** 043640
[44] Zhang Y C, Wang H T, Shen S Q and Liu W M 2013 *Chin. Phys. B* **22** 090501
[45] Wei X B, Meng Y M, Wu Z M and Gao X L 2015 *Chin. Phys. B* **24** 117101
[46] Xu H Y and Lai Y C 2020 *Phys. Rev. Research* **2** 013062
[47] Gennes P G de 1999 *Superconductivity of Metal and Alloys* (Westview Press)
[48] Zheng D, Zhang G M and Wu C 2011 *Phys. Rev. B* **84** 205121
[49] Semenoff G W, and Zhou F 2008 *Phys. Rev. Lett.* **101** 087204
[50] He L, Wang J, Peng S G, Liu X J and Hu H 2016 *Phys. Rev. Res.* **94** 043624
[51] Zhang Y C, Ding S and Zhang S 2017 *Phys. Rev. A* **95** 041603
[52] Wu Y R, Zhang X F, Liu C F, Liu W M and Zhang Y C 2021 *Superfluid Density and Collective Modes of Fermion Superfluid in Dice Lattice*
[53] Peotta S and Törmä P 2015 *Nat. Commun.* **6** 8944
[54] Hazra T, Verma N and Mohit Randeria M 2019 *Phys. Rev. X* **9** 031049
[55] Julku A, Peltonen T J, Liang L, Heikkilä and Törmä P 2020 *Phys. Rev. B* **101** 060505